JOURNAL OF SOLID STATE CHEMISTRY 5, 410–418 (1972)

Intermediate Fluorite-Related Phases in the Y_2O_3–YF_3 System—Examples of One-Dimensional Ordered Intergrowth

A. W. MANN AND D. J. M. BEVAN

School of Physical Sciences, The Flinders University of South Australia, Bedford Park, South Australia 5042

Received January 31, 1972

The composition region $YX_{2.13(0)}$–$YX_{2.22(0)}$ (X = O + F) of the Y_2O_3–YF_3 system has been examined in detail, and X ray single crystal and powder data for 11 discrete orthorhombic phases was collected. These orthorhombic phases, all closely related to one another and to the parent fluorite-type structure, can be accounted for on the basis of one-dimensional ordered intergrowth of basic orthorhombic unit cells, members n = 8, 7, 6, 5, and 4 of the homologous series $(Y_nO_{n-1}F_{n+2})_4$.

Introduction

The Y_2O_3–YF_3 system was first described by Zachariasen (*1*). He found only two intermediate phases, the rhombohedral stoichiometric compound YOF and a tetragonal nonstoichiometric phase $YX_{2+\delta}$ ($X = O + F$: $0 < \delta < 0.40$), both structures being closely related to the fluorite type. It now appears, however, that tetragonal $YX_{2+\delta}$, as such, does not exist, except perhaps at higher temperatures. Instead, a distinct diphasic region was found to exist at room temperature between rhombohedral YOF and a fluorite-related orthorhombic phase of approximate composition $YX_{2.14}$ (*2*). This orthorhombic phase is, in fact, one of a sequence of extremely closely related orthorhombic phases occurring in the composition region $YX_{2.13(0)}$–$YX_{2.22(0)}$ (designated the "orthorhombic phases region"). The orthorhombic phase at $YX_{2.22(0)}$ apparently coexists with YF_3. Several of these orthorhombic phases have been described briefly in the earlier publication; the present paper discusses in detail the structures of these and some additional orthorhombic phases in the light of subsequent investigations in which both powder and single crystal X ray diffraction techniques were used.

Experimental Methods

Some 36 samples in the composition range $YX_{2.10(0)}$–$YX_{2.30(0)}$ have now been prepared as physical mixtures of the desired weights of Y_2O_3 (99.99%) and YF_3 (99.9%). These samples were either pelleted and heated under an atmosphere of nitrogen or sealed into platinum capsules, heated to temperatures of 1000–1500°C for at least 24 hr, and subsequently cooled to room temperature over periods of time varying from approximately 1 min to several weeks. All samples were found to be highly crystalline. Three additional samples were obtained as products from fluxed melt preparations, and were in the form of crystals up to 0.5 cm in length. Analyses for fluorine and oxygen were carried out on samples subsequent to their heat treatment in a pyrohydrolysis apparatus similar to that described by Warf, Cline, and Tevebaugh (*3*).

Where possible, a combination of single-crystal and powder X ray techniques has been used to characterize the unknown intermediate phases. Table I contains a list of 11 such phases where single crystals of a sufficient size for study could be found. Powder data were obtained with a Hagg-Guinier focusing camera and monochromatic CuK_{α_1} radiation. Films were measured with a Pye two-dimensional traveling microscope accurate to ±0.001 cm, and in all cases an internal standard, ThO_2 (a_0 = 5.5969 Å), was used. Single crystal data were obtained with a Nonius Weissenberg camera by the equi-inclination technique. Films were again measured with the two-dimensional traveling microscope and, where necessary, corrections for film shrinkage and misalignment were determined from a compari-

TABLE I

PHASE DATA FOR SAMPLES INVESTIGATED BY POWDER AND SINGLE CRYSTAL DIFFRACTION

Composition	Phase analysis	Fluorite-type subcell parameters (±0.001 Å)		
		a_F	b_F	c_F
$YX_{2.13(6)}$[f]	orthorhombic phase	5.425	5.508	5.527
$YF_{2.11(5)}$	YOF + orthorhombic phase	5.420	5.512	5.527
$YX_{2.14(8)}$[f]	orthorhombic phase	5.419	5.519	5.529
$YX_{2.14(9)}$	orthorhombic phase	5.419	5.516	5.527
$YX_{2.16(5)}$	orthorhombic phase	5.416	5.520	5.528
$YX_{2.17(1)}$	orthorhombic phase	5.413	5.52(8)	5.52(8)
$YX_{2.18(3)}$[f]	orthorhombic phase	5.410	5.53(3)	5.53(3)
$YX_{2.18(7)}$	orthorhombic phase	5.407	5.53(3)	5.53(3)
$YX_{2.22(0)}$	YF_3 + orthorhombic phase	5.402	5.451	5.535
$YX_{2.22(5)}$	YF_3 + orthorhombic phase	5.400	5.544	5.534
$YX_{2.25(9)}$	YF_3 + orthorhombic phase	5.399	5.546	5.535

[f] = fluxed melt preparations.

son of the d^* spacings for the intense fluorite-type reflections with those calculated from the corresponding powder pattern.

Results

Fluorite-Type Subcells

All the diffraction patterns are very obviously fluorite-related (see Fig. 1). In fact, if weak superstructure lines are ignored, powder patterns of all intermediate phases can be indexed on a simple distorted fluorite-type subcell. The parameters of these subcells, for which both types of X ray data are available, are shown in Table I. At compositions towards the extremities of the "orthorhombic phases region" the fluorite-type subcells are obviously orthorhombic, while towards the center of the region their apparent tetragonality is due to a "crossover" in the relative lengths of the orthorhombic b and c parameters.

Basic Orthorhombic Unit Cells

The single crystal and Guinier powder patterns of $YX_{2.11(5)}$ and $YX_{2.16(5)}$ have been indexed completely. The true orthorhombic unit cell of $YX_{2.16(5)}$ designated the 7F unit, has the dimensions shown in Table II, and consists in essence of a stack of seven fluorite-type cubes piled one upon the other in the b-axis direction. The ideal composition of this phase is $Y_7O_6F_9(YX_{2.143})$, the contents of the unit cell being $(Y_7O_6F_9)_4$, and the space group *Abm*2. Figure 2 shows the zero-layer Weissenberg pattern. The full structure will be reported in a subsequent publication. Interstitial anions, presumably fluorines, are accommodated in the predominantly fluorite-type structure in layers parallel to (010), and are separated by $b/2$. Each individual interstitial anion is at a position close to, but significantly removed from, a vacant octahedral site in the fluorite-type structure. The distortion of the fluorite-type cubes immediately surrounding these sites is large; on the other hand, distortion of fluorite-type cubes is minimal at positions midway between the layers of interstitial atoms. At positions in the unit cell between these two extremes a gradual transition from distorted to virtually undistorted fluorite-type structure takes place. This phase is designated 7F, according to the unit cell length (of the b axis) expressed in terms of the number of fluorite-type subcells.

The data from $YX_{2.16(5)}$ (the single crystal data were obtained from a twinned crystal) show unambiguously that the orthorhombic unit cell (designated 6F) is made up of six fluorite-type cubes stacked along the b-axis; its cell parameters are given in Table II, and the ideal composition is $Y_6O_5F_8$ ($YX_{2.167}$). The close similarities between the diffraction data from this and the 7F phase suggest that essentially the same structural features obtain in both.

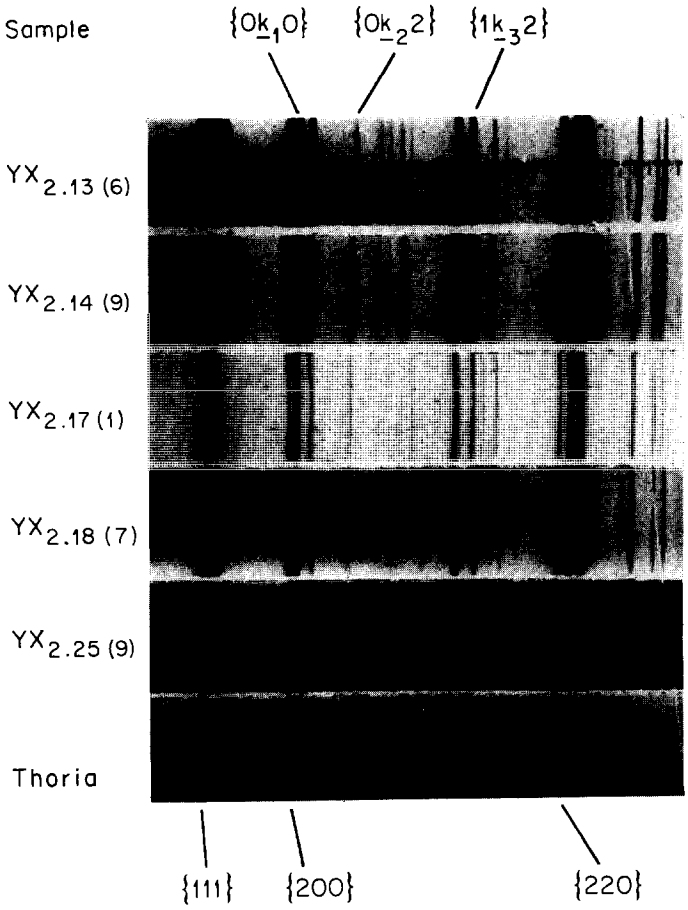

FIG. 1. Powder patterns of selected phases in the "orthorhombic phases region." Shifts in the positions of superstructure reflections $\{0k_2 2\}$ and $\{1k_3 2\}$ with changes in composition are evident.

The simple orthorhombic phase $Y_5O_4F_7$-($YX_{2.200}$), which should exist as a stable room temperature entity, has not yet been observed, probably because this exact composition has yet to be achieved. However, samples at compositions close to $YX_{2.200}$ (and samples in the Er–O–F system at close to $ErX_{2.200}$) give single-crystal and powder patterns which may very nearly be

TABLE II

BASIC UNIT ORTHORHOMBIC PHASES

Unit	Ideal composition	Formula	Unit cell parameters			
			a	*b*		*c*
8F	$YX_{2.125}$	$(Y_8O_7F_{10})_4 = Y_8X_{17}$	Not stable as a discrete entity			
7F	$YX_{2.143}$	$(Y_7O_6F_9)_4 = Y_7X_{15}$	5.420	38.58[a]	(=7 × 5.512)	5.527[a]
6F	$YX_{2.167}$	$(Y_6O_5F_8)_4 = Y_6X_{13}$	5.416	33.12	(=6 × 5.520)	5.520
5F	$YX_{2.200}$	$(Y_5O_4F_7)_4 = Y_5X_{11}$	5.406	27.69	(=5 × 5.538)	5.532
4F	$YX_{2.250}$	$(Y_4O_3F_6)_4 = Y_4X_9$	Not stable as a discrete entity			

[a] Originally reported as $c = 38.58$ Å, $b = 5.526$ Å. This designation has been interchanged in accordance with the structural findings.

FIG. 2. Zero-layer Weissenberg pattern of $YX_{2.11(5)}$ crystal (the 7F basic unit). Superstructure reflections are separated by one seventh of the distance between fluorite-type subcell reflections.

indexed on the basis of such a unit cell. In fact, the likely unit cell parameters of this phase may be obtained by a very small interpolation of the orthorhombic fluorite-type subcell parameters of neighboring phases; the parameters so obtained for this phase (5F) are included in Table II.

These three phases, 7F, 6F, 5F, are members of a simple homologous series $(Y_nO_{n-1}F_{n+2})_4$, where $n = 7, 6, 5$. The members $n = 8$, $(Y_8O_7F_{10})_4$, and $n = 4$, $(Y_4O_3F_6)_4$, of this same homologous series are outside the composition limits of the orthorhombic phases region and are therefore unobservable. However, their potential existence becomes important in any discussion of the structures of the complex orthorhombic phases which occur at and near the extremities of the orthorhombic phases region.

Ordered Intergrowth of Basic Units

At compositions between those of the simple homologues, the powder and single crystal X ray diffraction data have confirmed the existence of single discrete phases; diphasic patterns have never been observed within the orthorhombic phases region. The powder patterns of these phases, some of which are shown in Fig. 1, are all very similar and quite obviously fluorite-related; it is easy to see why previous results were interpreted as indicating a tetragonal phase of wide homogeneity range. Small but very significant differences between powder patterns are, however evident. For example, the positions in different films of superstructure reflections marked $\{0k_22\}$ and $\{1k_32\}$ in Fig. 1 vary monotonically with composition. The amount of shift across any part of the range is, however, far greater than the corresponding shift in position of any neighboring intense fluorite-type reflection, and cannot be accounted for merely in terms of changes in the parameters of the average unit cell of a non-stoichiometric phase with changing composition. These two particular superstructure reflections appear in, and have been indexed for, powder patterns of the basic unit phases 7F, 6F, and it is the values of k_2 and k_3, respectively, which change with changing composition.

Each intermediate phase also exhibits a unique single-crystal diffraction pattern, from which much structural information can be derived; Figs. 2, 3, 4, 5 contain patterns of some representative phases. For example, between successive intense fluorite-type reflections in the pattern of $YX_{2.18(7)}$ (Fig. 3) four groups of superstructure reflections occur, dividing the reciprocal lattice intervals of the fluorite-type subcell roughly into fifths (NB, the composition of $YX_{2.18(7)}$ is close to that for the 5F structure). The exact identity of the unit cell is not however 5F, because each superstructure group, and indeed each fluorite-type reflection, is distinctly split: Figure 4 shows some of these superstructure groups from $YX_{2.18(7)}$ under higher magnification. Reciprocal lattice distances between these very close "super-superstructure" reflections are measurably different in films of neighboring phases, even for samples extremely close in composition, e.g., compare Fig. 3, the single crystal pattern for sample $YX_{2.18(7)}$ with Fig. 5, that for sample $YX_{2.18(3)}$.

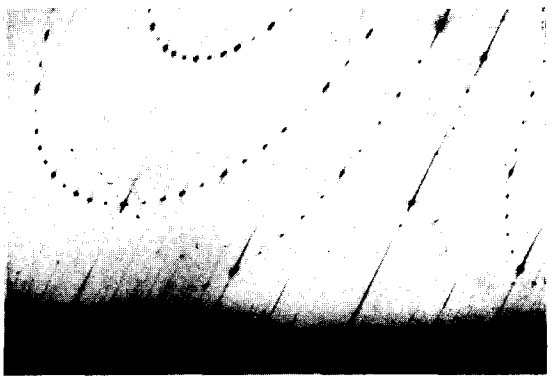

FIG. 3. Zero-layer Weissenberg pattern of $YX_{2.18(7)}$ crystal (317 Å *b*-axis). Superstructure reflections occur in groups separated by approximately one fifth of the distance between fluorite-type subcell reflections.

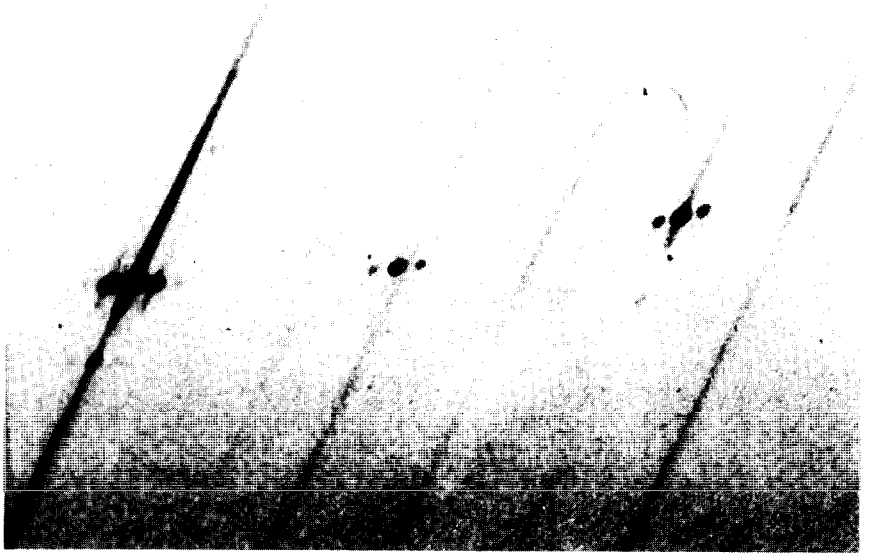

FIG. 4. Portion of Fig. 3 magnified.

Overall, these powder and single-crystal data can be rationalized in terms of a structural model in which two kinds of basic unit are interspersed and intergrown in a regular manner; logically, this will occur as stacking of basic units with (010) faces common, to create one-dimensional long-period superstructures.

Powder Pattern Analysis

Two of the superstructure reflections apparently common to all phases, and referenced as $\{0k_2 2\}$ and $\{1k_3 2\}$ reflections in the powder patterns shown in Fig. 1, have been indexed for the 7F and 6F (also for the calculated[1] 5F unit) basic unit phases. The indices assigned to these two reflections, and to the nearby reflection $\{0k_1 0\}$ (which is the reflection corresponding to fluorite {020}), in each basic unit phase, are shown in Table III.

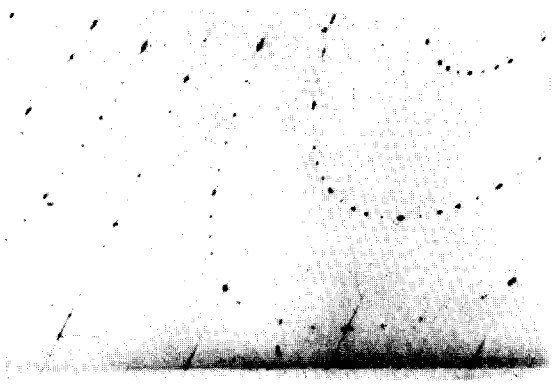

FIG. 5. Zero-layer Weissenberg pattern of $XY_{2.18(3)}$ crystal (252 Å *b*-axis). Superstructure reflections occur in groups separated by approximately one fifth of the distance between fluorite-type subcell reflections.

Similarities between the indices required in each of the indexings are evident; only the k index for each reflection differs from phase to phase. If n is used to denote the number of fluorite-type cubes in each basic unit, then the reflections $\{0k_1 0\}$, $\{0k_2 2\}$, and $\{1k_3 2\}$ may be written respectively as $\{0(2n)0\}$, $\{0(n-1)2\}$, and $\{1(n+1)2\}$. The last two (superstructure) reflections correspond to diffraction from very similar planes in each of the three basic units, planes with spacings becoming increasingly different from those of the ideal fluorite-type {012} and {112} planes, respectively, as the value of n decreases. These same two superstructure reflections are those for which a large yet consistent shift in $\sin^2\theta$ values with composition was observed across the entire orthorhombic phases region; their $\sin^2\theta$ values in the 7F, 6F, and 5F phases conform to the general trend.

[1] By interpolation of $\sin^2\theta$ values from patterns at nearby compositions.

TABLE III

$\sin^2\theta$ AND $\{hkl\}$ VALUES FOR $\{0k_1\}$, $\{0k_22\}$, AND $\{1k_32\}$ REFLECTIONS

Basic unit	$\{0k_10\}$ (Fluorite-type)		$\{0k_22\}$ (Superstructure)		$\{1k_32\}$ (Superstructure)	
	$\sin^2\theta$	$\{hkl\}$	$\sin^2\theta$	$\{hkl\}$	$\sin^2\theta$	$\{hkl\}$
7F	0.07811	{0(14)0}	0.09199	{062}	0.12359	{182}
6F	0.07786	{0(12)0}	0.09125	{052}	0.12430	{172}
5F	0.07750[a]	{0(10)0}	0.08995[a]	{042}	0.12568[a]	{162}

[a] By interpolation of $\sin^2\theta$ values from patterns at nearby compositions.

Intuitively, the same correlations should apply to the intermediate phases as well.

In the orthorhombic system

$$\sin^2\theta_{\{hkl\}} = h^2\,\mathrm{A} + k^2\,\mathrm{B} + l^2\,\mathrm{C}$$

(where

$$\mathrm{A} = \frac{\lambda^2}{4a^2},\quad \mathrm{B} = \frac{\lambda^2}{4b^2},\quad \mathrm{C} = \frac{\lambda^2}{4c^2}\Big)$$

Thus for the $\{0k_10\}$ reflection:

$$\sin^2\theta_{\{0k_10\}} = k_1{}^2\mathrm{B}$$

for the $\{0k_22\}$ reflection:

$$\sin^2\theta_{\{0k_22\}} = k_2{}^2\,\mathrm{B} + 4\mathrm{C}$$

and for the $\{1k_32\}$ reflection:

$$\sin^2\theta_{\{1k_32\}} = 1\mathrm{A} + k_3{}^2\,\mathrm{B} + 4\mathrm{C}$$

In these expressions the values of A and C are determined quite precisely from the a and c parameters of the fluorite-type subcells (see Table I) since, for any given intermediate phase, these are unaffected by an uncertainty in the number of subcells comprising the one-dimensional (b-axis) superstructure cell.

It then follows that two ratios, R_1 and R_2, can be defined such that

$$R_1 = \frac{k_1{}^2}{k_2{}^2} = \frac{\sin^2\theta_{\{0k_10\}}}{\sin^2\theta_{\{0k_22\}} - 4\mathrm{C}}$$

and

$$R_2 = \frac{k_1{}^2}{k_2{}^2} = \frac{\sin^2\theta_{\{0k_10\}}}{\sin^2\theta_{\{1k_32\}} - \mathrm{A} - 4\mathrm{C}}$$

These ratios, R_1 and R_2, can therefore be obtained directly by experiment for each intermediate phase. These may be matched with theoretically calculated ratios of the type $(N^2/N_1{}^2)$ and $(N^2/N_2{}^2)$ (N, N_1, N_2 integers) to obtain values for k_1, k_2, and k_3 of the three reflections. The reflections $\{0k_10\}$ correspond to the {020} reflections from a fluorite subcell; the unit-cell length of the true cell is then given directly since $n = k_1/2 = N/2$. In practice, several (unrelated) pairs of values for $N^2/N_1{}^2$ and $N^2/N_2{}^2$ were found to satisfy the experimentally determined ratios R_1 and R_2 to within their experimental error of $\pm 1\%$.

Single-Crystal Pattern Analysis

For most of the intermediate phases, reciprocal lattice (d^*) spacings between successive superstructure reflections on the zero-layer festoons permit the true b to be calculated directly (*4*), i.e., $b = \lambda/d^*$. Evidence from the simple 7F and 6F structures suggests, however, that only those reflections with even values of k may be present on zero-layer photographs; this is certainly true for a side-centered (odd n) intermediate phase, but not necessarily for those phases with an even number of fluorite-type subcells in the unit cell. For simplicity it is assumed that only even values of k are observed, i.e., that $b = 2\lambda/d^*$; for even-numbered cells so derived, the possible existence of the smaller unit cell must be kept in mind.

The error associated with measurements on these single-crystal films is approximately $\pm 4\%$. This means that calculations for n (the number of fluorite-type subcells in the unit cell), which can be made by dividing the true unit cell length b of the intermediate phase by b_F, the fluorite-type subcell lattice parameter found from powder data, will not be unambiguous for values of $b > 50$ Å.

Combination of Powder and Single-Crystal Data

For intermediate phases of any complexity, neither powder data nor single-crystal data

TABLE IV

UNIT CELLS FOR INTERMEDIATE PHASES[a]

Sample	Derived unit cell n	Powder pattern ratios		Unit cell b (Å)	
		Experimental	Derived cell	Experimental	Derived cell
$YX_{2.13(6)}$[f]	23F	$R_1 = 5.25 \pm 0.06$	5.29	128 ± 5	126.7
		$R_2 = 3.11 \pm 0.03$	3.13		
$YX_{2.11(5)}$	7F	$R_1 = 5.46 \pm 0.06$	5.44	38.5 ± 2	38.6
		$R_2 = 3.04 \pm 0.03$	3.06		
$YX_{2.14(8)}$[f]	19F	$R_1 = 5.66 \pm 0.06$	5.64	105 ± 5	104.9
		$R_2 = 2.98 \pm 0.03$	2.98		
$YX_{2.14(9)}$	45F	$R_1 = 5.58 \pm 0.06$	5.61	248 ± 10	248.2
		$R_2 = 3.00 \pm 0.03$	3.00		
$YX_{2.16(5)}$	6F	$R_1 = 5.72 \pm 0.06$	5.76	33 ± 1	33.1
		$R_2 = 2.94 \pm 0.03$	2.94		
$YX_{2.17(1)}$	17F	$R_1 = 5.90 \pm 0.06$	5.90	91 ± 4	94.0
		$R_2 = 2.90 \pm 0.03$	2.89		
$YX_{2.18(3)}$[f]	47F	$R_1 = 6.08 \pm 0.06$	6.12	252 ± 10	260.0
		$R_2 = 2.82 \pm 0.03$	2.82		
$YX_{2.18(7)}$	57F	$R_1 = 6.16 \pm 0.06$	6.14	317 ± 12	315.4
		$R_2 = 2.80 \pm 0.03$	2.81		
$YX_{2.22(0)}$	28F	$R_1 = 6.42 \pm 0.06$	6.48	155 ± 6	155.2
		$R_2 = 2.73 \pm 0.03$	2.71		
$YX_{2.22(5)}$	28F	$R_1 = 6.45 \pm 0.06$	6.48	157 ± 6	155.2
		$R_2 = 2.71 \pm 0.03$	2.71		
$YX_{2.25(9)}$	41F	$R_1 = 6.54 \pm 0.06$	6.51	222 ± 9	227.4
		$R_2 = 2.69 \pm 0.03$	2.69		

[f] = fluxed melt preparations.

[a] However, for $YX_{2.22(0)}$ and $YX_{2.22(5)}$ both with the same (28F) unit cell, a unit with half the indicated b-axis (i.e., 14F) must also be considered, but for the structural interpretation of this intermediate phase, the ambiguity is, at this stage, trivial.

alone are sufficient to establish a unique unit cell, but for each intermediate phase so far investigated *only one cell has been found to satisfy both sets of data simultaneously.*

The unique unit cells are shown in Table IV. The same technique applied to $YX_{2.11(5)}$ and $YX_{2.16(5)}$ illustrates the generality of the method even for basic unit phase determination.

Interpretation of Results

One test of the ordered intergrowth description of the intermediate phases is based on two experimentally determined properties: (a) the unit cell length n; and (b) the analyzed composition of each phase, although for several diphasic samples at the extremities of the orthorhombic phases region this latter can only be estimated from an overall sample composition.

The property (a) is particularly significant if the proportions of adjacent basic units in any intergrowth phase are to be assigned, as indeed they must be for such a description to hold. When the analyzed composition is also taken into account, it is found that all nine intermediate phases so far studied can be described in terms of ordered intergrowth of basic units, and of these, only the two longest supercells, 47F and 57F, have possible alternative intergrowth proportions. The intergrowth models proposed are shown in Table V.

Included in Table V for each phase are the values of the integers in the theoretical ratios N^2/N_1^2 and N^2/N_2^2 used to match R_1 and R_2, These are the k indices assigned to the powder pattern reflections $\{0k_10\}$, $\{0k_22\}$, and $\{1k_32\}$ whose $\sin^2\theta$ values defined R_1 and R_2. As already stated, these same reflections in the basic unit

TABLE V

ORDERED INTERGROWTH MODELS

Composition	Unit	Ordered intergrowth	Calculated composition	k indices from theoretical ratios		
				k_1	k_2	k_3
$YX_{2.13(6)}$[f]	23F	2 × (8F) + 1 × (7F)	$YX_{2.130}$	46	20	26
$YX_{2.11(5)}$	7F	1 × (7F)	$YX_{2.143}$	14	6	8
$YX_{2.14(8)}$[f]	19F	1 × (7F) + 2 × (6F)	$YX_{2.153}$	38	16	22
$YX_{2.14(9)}$	45F	3 × (7F) + 4 × (6F)	$YX_{2.155}$	90	38	52
$YX_{2.16(5)}$	6F	1 × (6F)	$YX_{2.167}$	12	5	7
$YX_{2.17(1)}$	17F	2 × (6F) + 1 × (5F)	$YX_{2.176}$	34	14	20
$YX_{2.18(3)}$[f]	47F	2 × (6F) + 7 × (5F)	$YX_{2.191}$	94	38	56
		7 × (6F) + 1 × (5F)	($YX_{2.170}$)			
$YX_{2.18(7)}$	57F	2 × (6F) + 9 × (5F)	$YX_{2.193}$	114	46	68
		7 × (6F) + 3 × (5F)	($YX_{2.175}$)			
$YX_{2.22(0)}$	28F	4 × (5F) + 2 × (4F)	$YX_{2.214}$	56	22	34
$YX_{2.22(5)}$	28F	4 × (5F) + 2 × (4F)	$YX_{2.214}$	56	22	34
$YX_{2.25(9)}$	41F	5 × (5F) + 4 × (4F)	$YX_{2.220}$	82	32	50

[f] = fluxed melt preparations.

phases have the general indices $\{0(2n)0\}$, $\{0(n-1)2\}$, and $\{1(n+1)2\}$, respectively, where n is the number of fluorite-type subcells in the unit cell. For any intermediate phase formed by intergrowth of adjacent basic units (now designated n_1F and n_2F) interspersed in the ratio r_1/r_2 (where $r_1n_1 + r_2n_2 = n$), relationships of the type:

$$k_1 = r_1(2n_1) + r_2(2n_2)$$
$$k_2 = r_1(n_1 - 1) + r_2(n_2 - 1)$$
$$\text{and } k_3 = r_1(n_1 + 1) + r_2(n_2 + 1)$$

are found to exist, i.e., the k indices of these reflections in the intermediate phases are simply the appropriate combination of the k indices of corresponding reflections in the constituent basic unit phases. The result is perhaps not surprising, but it does illustrate the facility with which "ordered intergrowth" provides not only an interpretation of superstructure line positions, but also the exact indices required for a successful powder pattern indexing. For $YX_{2.18(3)}$ and $YX_{2.18(7)}$, (see Table V), only the first-listed model in each case provides k values which agree with those from the matching of theoretical ratios R_1 and R_2. (E.g., the values of k_1, k_2, and k_3 calculated from the above equations for the second alternative $YX_{2.18(3)}$ are 94, 39, and 55. These yield theoretical ratios of N^2/N_1^2 and N^2/N_2^2 which are not in agreement with the observed ratios R_1 and R_2).

Discussion

Intergrowth examples involving combinations of 4F with 5F, 5F with 6F, 6F with 7F, and 7F with 8F have all been observed. It is interesting to note that while large unit cells containing roughly equal proportions of constituent basic units (e.g., $YX_{2.25(9)}$ and $YX_{2.14(9)}$) show very little fine superstructure on single-crystal patterns (i.e., successive reflections are of widely differing intensity), large unit cells containing a high proportion of one basic unit type (e.g., $YX_{2.18(7)}$ and $YX_{2.18(3)}$) contain superstructure "groups" clearly indicative of the predominant basic unit. In these latter two examples it may be reasonable to regard the structure primarily as a modification of 5F structure by the inclusion of small amounts of 6F phase.

The terminal phases of the orthorhombic phases region have obviously not been clearly defined. At the low-anion limit, $YX_{2.13(6)}$ (grown from a fluxed melt) is found to have a higher proportion of member 8F and a correspondingly lower composition than $YX_{2.11(5)}$ obtained from an apparently diphasic mixture containing YOF as well. Samples $YX_{2.22(0)}$, $YX_{2.22(5)}$, and $YX_{2.25(9)}$ all contain orthorhombic phases in apparent equilibrium with YF_3, yet structurally and compositionally $YX_{2.22(5)}$, and $YX_{2.22(0)}$ are different from $YX_{2.25(9)}$. The answer to these problems is not yet clear. Although the terms

"gross sample inhomogeneity" and "nonequilibrium" most easily explain these phenomena, it is possible that more subtle explanations involving phase nucleation problems arising from minor variations in external physical factors at the time of crystallite formation may prove more realistic in these cases where compositional differences between phases are so small.

Perhaps the overall situation in the entire orthorhombic phases region is not as simple as this "unit cell" approach might suggest. Stacking sequences of the basic unit phases in the intermediate phase unit cells have yet to be determined; various types of *intergrowth irregularity* are possible which will maintain the apparent long-range order exhibited in X ray diffraction patterns of bulk crystal. What has been observed in any one of these X ray diffraction patterns is likely to prove to be an *average intergrowth periodicity*. The techniques of electron diffraction and microscopy, which have been so elegantly applied to alloy systems (*5*), the hexagonal ferrites (*6*), and systems exhibiting two-dimensional ordered intergrowth (*7–10*) have an important role to play in resolving these and other problems in the Y_2O_3–YF_3 system.

Acknowledgments

Our thanks are due to B. Wanklyn and L. Holst who, independently, supplied us with "fluxed melt" samples.

References

1. W. H. Zachariasen, *Acta Crystallogr.* **4**, 231 (1951).
2. D. J. M. Bevan, R. S. Cameron, A. W. Mann, G. Brauer and U. Roether, *Inorg. Nucl. Chem. Lett.* **4**, 241 (1968).
3. J. C. Warf, W. D. Cline and R. D. Tevebaugh, *Anal. Chem.* **26**, 342 (1954).
4. M. J. Buerger, "X-Ray Crystallography" p. 284. Wiley, London (1962).
5. M. Hirabayashi, S. Yamaguchi, K. Hiraga, N. Ino and H. Sato, *J. Phys. Chem. Solids* **31**, 77 (1970).
6. C. F. Cook, *J. Appl. Phys.* **38**, 2488 (1967).
7. J. G. Allpress, J. V. Sanders and A. D. Wadsley, *Acta Crystallogr., Sect. B.* **25**, 1156 (1969).
8. J. G. Allpress, J. V. Sanders and A. D. Wadsley, *J. Solid State Chem.* **1**, 28 (1969).
9. J. G. Allpress, *J. Solid State Chem.* **1**, 66 (1969).
10. J. G. Allpress, *Mater. Res. Bull.* **10**, 707 (1969).